Controlling the dynamics of dissipationless localized bound states in open quantum systems with periodic driving fields

Fei-Lei Xiong[1] and Wei-Min Zhang[1,2,*]

[1]*Department of Physics and Center for Quantum Information Science, National Cheng Kung University, Tainan 70101, Taiwan*
[2]*Physics Division, National Center for Theoretical Sciences, Taipei 10617, Taiwan*

In this paper, we study the exact dynamics of open quantum systems in the presence of dissipationless localized bound states and periodic driving fields. We show that different from the static adjustment of the system parameters to control the existence of localized bound states in open quantum systems, the periodic driving can either modulate the dynamics of the existing localized bound states or make some of them disappear due to the sideband generation from the driving that makes electrons transit between the localized bound states and continuous states. This analysis is also different from the widely used Floquet theory in the study of the driving effect on open system dynamics. We also find the conditions for the protection of the dissipationless localized bound states from the driving and for the manipulation of quantum coherence between localized bound states using the driving. The results for the dynamics of localized bound states have a potential application in controlling the quantum state against decoherence for the sake of its sensitivity to the fundamental frequency of the driving field and its strength.

I. INTRODUCTION

Quantum decoherence, which is ubiquitous in all kinds of physical systems, acts as a key obstacle in implementing novel quantum information protocols. As a consequence, ever since quantum information sciences were proposed, controlling quantum decoherence has been a lasting and hard topic [1]. After decades of study, the understanding of decoherence is now much deeper [2,3]. Physicists have gone far beyond the Born-Markov master equation [4], the Gorini–Kossakowski–Sudarshan (GKS)-Lindblad master equation [5,6], and the truncated Nakajima-Zwanzig master equation [7–9], which are either only applicable in the weak-coupling regime or just an approximation to the practically unsolvable formal equation. The exact master equations for quantum Brownian motion [10,11], for electronic and photonic open quantum systems [12–16], and for hybrid topological superconducting systems [17,18], as well as those that are mathematically equivalent to them, have been successfully derived.

In the past 10 years, we have systematically studied a large class of open quantum systems incorporating quantum transport (see the reviews [3,19] and the references therein) and have obtained the exact master equations as well as their solutions expressed in terms of the nonequilibrium Green's functions [12–16]. It has been proved that the existence of dissipationless localized bound states (localized modes) which are induced by the structured system-environment interactions [15] offers deep understanding of how the decoherence of open quantum systems can be suppressed with these localized bound states. They form a decoherence-free subspace without the additional requirement of symmetries and therefore have potential applications in practical quantum information storage and processing.

On the other hand, many methods to control decoherence, ever since the proposal of spin echoes [20,21], have been developed, such as the use of dynamical decoupling [22–27] and the introduction of spatial periodicity [28–33]. In addition to the above protocols, it has also long been confirmed that driving in the open systems can impose significant effects on decoherence [34–42]. It has been used to achieve quantum control and decoherence-rate manipulation of superconducting qubits [27,36,43,44] and quantum dots [40,45–48]. Theoretic methods of dealing with this problem, such as the spectral filtering theory [49–53] and those based on the Floquet theory [54–56], have also been proposed. Considering the possibility of localized bound states serving as quantum memory [42], localized bound states under periodic driving may also hold potential not only for quantum information processing against decoherence but also for quantum memory protocols.

In this paper, we shall focus on the quantum-dot-based quantum protocols which have been recognized as the earliest promising candidate for solid-state quantum computing [57,58]. Quantum-dot-based quantum computing has been developing quickly recently, and much progress has been made in it [45–48,59]. For example, all-electric control with high fidelity has been fulfilled by several groups [46,60–63], making the electron charge- and spin-state controls feasible in experiments. In this work, we shall extend our systematic works [12–16] on open quantum systems to the case in which time-periodic driving is exerted on the dissipationless localized bound states in such systems. We analyze the influences of the driving field on the dynamics of localized bound states based on the theoretical analysis and also numerical calculations. The framework is based on the picture of electron

transition and energy transfer between the localized bound state and the continuous states induced by the driving in the real-time domain. It is different from the Floquet theory [41,54–56] and also different from the theory given in Ref. [40] except for the sideband generation.

The rest of the paper is organized as follows. In Sec. II, we introduce the system with which we are concerned and the general framework we use for the study of decoherence dynamics through the nonequilibrium Green's functions that was obtained in our exact master-equation formalism. We analyze the major effects of the driving field applied to open quantum systems in general and the dynamical influence on the localized bound states of open quantum systems in particular in this section. It shows that the driving applied to the system can induce multiple electron transitions between the localized bound states and the scattering modes as a consequence of sideband generation. In Sec. III, we numerically study the decoherence dynamics of the open quantum system under weak periodic driving and theoretically analyze various possible changes to the decoherence dynamical properties induced by the driving. We show that periodic driving can usually generate sidebands and then induce electrons in the dissipationless localized bound state to dissipate as well. However, by properly adjusting the frequencies of the periodic driving field, such dissipation can be avoided, and quantum coherence between localized bound states can be generated. Section IV shows that when the driving field becomes strong, the dynamical features demonstrated by the weak periodic driving can be significantly enhanced. The conclusion and potential applications are given in Sec. V.

II. THE GENERAL FORMALISM

We shall focus on a class of electronic open quantum systems driven by a periodic external field. An exemplary schematic setup of such a device is demonstrated in Fig. 1(a). For the sake of simplicity and without loss of generality, we consider the system containing only a single energy level. The general formulation dealing with the exact dynamics of such systems can be found in our previous works [13,15]. The corresponding total Hamiltonian can be modeled as

$$H_{\text{tot}}(t) = [\epsilon_s + \epsilon_d(t)]b^\dagger b + \sum_{\alpha k} \epsilon_{\alpha k} b_{\alpha k}^\dagger b_{\alpha k}$$
$$+ \sum_{\alpha k} (V_{\alpha k} b^\dagger b_{\alpha k} + \text{H.c.}). \quad (1)$$

The first term is the system Hamiltonian in which ϵ_s is the system on-site energy; $\epsilon_d(t)$ is an external periodic driving field acting as the time-dependent potential of the central island (quantum dot) with fundamental period T, $\epsilon_d(t + T) = \epsilon_d(t)$; and b ($b^\dagger$) is the electron annihilation (creation) operator of the system. The second term is the environment Hamiltonian, where $\epsilon_{\alpha k}$ is the single-particle energy of mode k in reservoir α; in addition, $b_{\alpha k}$ and $b_{\alpha k}^\dagger$ are the corresponding electron annihilation and creation operators in the reservoir, respectively. The last term is the system-reservoir coupling, with $V_{\alpha k}$ standing for the coupling strength between the system and mode k of reservoir α. Equation (1) is also a prototype in mesoscopic physics that describes the quantum transport of
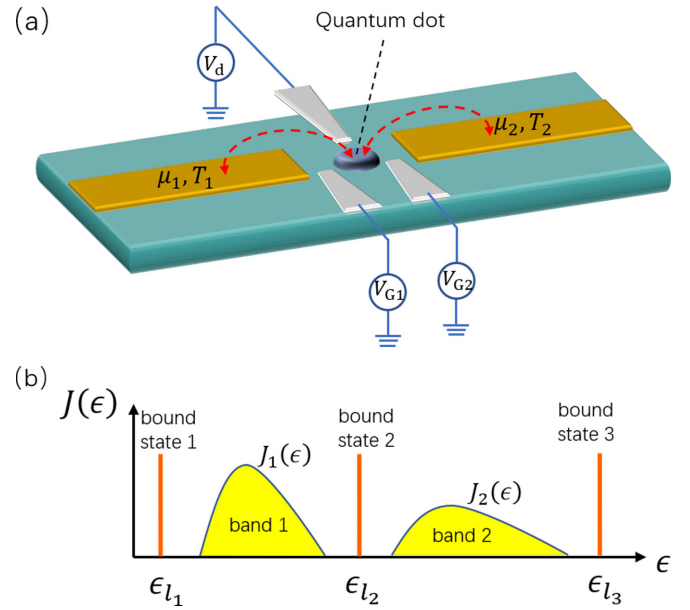

FIG. 1. (a) Schematic setup of the quantum-dot device described by Eq. (1), with the two leads serving as the two reservoirs $\alpha = 1, 2$. The energy level of the quantum dot can be tuned through the dot gate V_d. The coupling strengths between the quantum dot and leads are also controllable through gates V_{G1} and V_{G2}. The bias voltage V_{BS} to the two leads can tune the chemical potentials (Fermi surfaces) of two leads. As we show, with the transformation of Eq. (4), the dynamics of quantum-dot system with the driving field applied to the leads or to the gates V_{G1} and V_{G2} is equivalent to the driving applied to the dot gate described by Eq. (2). (b) Schematic plot of the spectral densities (associated with the two leads and their couplings with the central quantum dot) and the possibly present localized bound states. When the two spectral densities overlap, the localized bound state ϵ_{l_2} cannot occur.

a single-level quantum dot coupled to several leads, and the driving field $\epsilon_d(t)$ can be conveniently implemented by exerting a time-dependent gate voltage on the quantum dot [19,64]. As we shall show next, the driving field can also be applied to the reservoirs or the tunneling barriers between the system and the reservoirs, for which the resulting dynamics of the quantum systems are equivalent.

Based on the exact master-equation formalism [12–16], the decoherence dynamics of the system can be simply explored by the damping behavior of the spectral Green's function $u(t, t_0) = \langle \{b(t), b^\dagger(t_0)\} \rangle$, where $b(t)$ and $b^\dagger(t_0)$ are operators in the Heisenberg picture and $\{\cdot, \cdot\}$ denotes the anticommutator. Following the equation of motion approach, it is easier to find that $u(t, t_0)$ satisfies the integro-differential equation [12]

$$\frac{d}{dt}u(t, t_0) + i[\epsilon_s + \epsilon_d(t)]u(t, t_0) + \int_{t_0}^t d\tau\, g(t, \tau)u(\tau, t_0) = 0, \quad (2)$$

subjected to the initial condition $u(t_0, t_0) = 1$. Here, $g(t, \tau) = \int \frac{d\epsilon}{2\pi} J(\epsilon)e^{-i\epsilon(t-\tau)}$ is the time correlation function between the system and the reservoirs, and $J(\epsilon) = 2\pi \sum_{\alpha=1,2;k} |V_{\alpha k}|^2 \delta(\epsilon - \epsilon_{\alpha k}) \to J_1(\omega) + J_2(\omega)$ specifies the corresponding spectral densities shown in Fig. 1(b). In our exact master-equation formalism [3,12–15], it is shown that

the dissipation dynamics (or the relaxation dynamics) is fully determined by the time-dependent dissipative rate:

$$\gamma(t, t_0) = -\text{Re}\left[\frac{d}{dt}\ln u(t, t_0)\right]. \quad (3)$$

Thus, how the decoherence dynamics is controlled by the driving is completely described by the time evolution of $u(t, t_0)$.

Furthermore, if we make a transformation,

$$u(t, t_0) = u'(t, t_0)\exp\left\{-i\int_{t_0}^t dt'\epsilon_d(t')\right\}, \quad (4)$$

then one can find from Eq. (2) that

$$\frac{d}{dt}u'(t, t_0) + i\epsilon_s u'(t, t_0) + \int_{t_0}^t d\tau g'(t, \tau)u'(\tau, t_0) = 0, \quad (5)$$

where $g'(t, \tau) = g(t, \tau)\exp\{i\int_\tau^t dt'\epsilon_d(t')\}$. Equation (5) describes the decoherence dynamics of the same system, but the driving field is now applied to the leads directly, i.e., $\epsilon_{\alpha k} \to \epsilon_{\alpha k} - \epsilon_d(t)$ [13], which has often been used in the manipulation of electron charge and spin states in quantum-dot-based quantum computing devices [45–48,59–63]. Meanwhile, Eq. (5) with the above two-time correlation function $g'(t, \tau)$ between the system and the reservoirs also corresponds to a special driving field (such as periodic kick pulses) being applied directly to the tunneling barriers between the system and the reservoirs for the electron transport manipulation in the experiments [65–68]. This shows that the Green's function of Eq. (2) with a simple driving field possesses the universality for several different control manners of decoherence dynamics in electronic open systems.

The periodic driving field $\epsilon_d(t)$ can be separated into two parts. One is of average strength, and the other is time dependent and of zero-average in a period T, i.e.,

$$\epsilon_d(t) = \overline{\epsilon}_d + \delta\epsilon_d(t), \quad (6)$$

with $\overline{\epsilon}_d = \frac{1}{T}\int_t^{t+T} d\tau\epsilon_d(\tau)$. Actually, the first part $\overline{\epsilon}_d$ can be simply counted as the system on-site energy modulation. Without the $\delta\epsilon_d(t)$ part, the tuning of $\overline{\epsilon}_d$ can make the open system generate localized bound states [15]. Explicitly, for vanishing $\delta\epsilon_d(t)$, the spectral Green's function is denoted as $u_0(t, t_0)$, which satisfies the equation

$$\frac{d}{dt}u_0(t, t_0) + i[\epsilon_s + \overline{\epsilon}_d]u_0(t, t_0) + \int_{t_0}^t d\tau g(t, \tau)u_0(\tau, t_0) = 0. \quad (7)$$

The exact solution of $u_0(t, t_0)$ has the analytic form [15]

$$u_0(t, t_0) = \int\frac{d\epsilon}{2\pi}D(\epsilon)e^{-i\epsilon(t-t_0)}, \quad (8)$$

where $D(\epsilon)$ is the modification of the system energy level as a combined contribution from the coupling to the reservoir and from the static part $\overline{\epsilon}_d$ of the driving field. The form of $D(\epsilon)$ is given explicitly by

$$D(\epsilon) = 2\pi\sum_i Z_i(\epsilon)\delta(\epsilon - \epsilon_{l_i})$$
$$+ \frac{J(\epsilon)}{[\epsilon - (\epsilon_s + \overline{\epsilon}_d) - \Delta(\epsilon)]^2 + J^2(\epsilon)/4}, \quad (9)$$

where $\Delta(\epsilon) = \text{P}[\int\frac{d\epsilon'}{2\pi}\frac{J(\epsilon')}{\epsilon-\epsilon'}]$ is the self-energy correction to the system, with P denoting the principal value of the integral, $\Sigma(\epsilon) = \int\frac{d\epsilon'}{2\pi}\frac{J(\epsilon')}{\epsilon-\epsilon'+i0^+} = \Delta(\epsilon) - \frac{i}{2}J(\epsilon)$ being the self-energy correction of the system, and $Z_i(\epsilon) = [1 - \Sigma'(\epsilon)]^{-1}$.

Obviously, Eq. (8) contains two contributions, the dissipationless oscillations arising from the localized bound states with energies ϵ_{l_i} and the nonexponential decays arising from the energy-level broadening [15]. The localized bound state arises from the energy shift contributed by the coupling between the system and the environment as well as the static part $\overline{\epsilon}_d$ of the driving field. The total energy shift pushes the renormalized energy of the system to allocate in the band gaps or in the vanishing frequency regimes of the spectral density such that the renormalized energy obeys the following condition [15]:

$$\epsilon_{l_i} - (\epsilon_s + \overline{\epsilon}_d) - \Delta(\epsilon_{l_i}) = 0, \quad J(\epsilon_{l_i}) = 0. \quad (10)$$

Such renormalized energy states become effectively decoupled from the environment and therefore become dissipationless or decoherence free; see the schematic plot of the spectral densities and the possible localized bound states in Fig. 1(b).

The existence of localized bound states can be manipulated by the modulation of the system on-site energy through the static part $\overline{\epsilon}_d$ of the driving field to satisfy Eq. (10). In other words, one can control the static part of the driving field to generate localized bound states and thereby suppress decoherence. Also note that if the system couples to multiple reservoirs, the above concept of dissipationless localized bound states can be directly applied to the case of a system coupled to multiple reservoirs. This is because the total spectral density is just the summation of the spectral densities of all reservoirs, as shown after Eq. (2).

In the following sections, we shall demonstrate that the time-dependent part $\delta\epsilon_d(t)$ plays an intrinsically different role in modulating the system dynamics in comparison with that given by the static part $\overline{\epsilon}_d$. To illustrate the effect of $\delta\epsilon_d(t)$ in the driving field more clearly, we transform the total Hamiltonian to a new basis. Formally, the time-independent part of the total Hamiltonian can be diagonalized. Without loss of generality, we may consider only one reservoir, namely, a dot system coupled to a single lead [69,70], so that the index α in Eq. (1) can be dropped. The relation between the diagonalized eigenmodes and the original modes of the Hamiltonian reads [42,71,72]

$$c_l^\dagger = \sqrt{Z_l}b^\dagger + \sqrt{Z_l}\sum_k\frac{V_k}{\epsilon_l - \epsilon_k}b_k^\dagger, \quad (11a)$$

$$c_k^\dagger = b_k^\dagger + V_k U(\epsilon_k)\left[b^\dagger + \sum_{k'}\frac{V_{k'}}{\epsilon_k - \epsilon_{k'} + i0}b_{k'}^\dagger\right], \quad (11b)$$

where $c_l^\dagger$ and $c_k^\dagger$ are the creation operators of the lth localized bound state and scattering mode k, respectively, and $U(\epsilon_k) = 1/[\epsilon_k - (\epsilon_s + \overline{\epsilon}_d) - \Sigma(\epsilon_k)]$ is the spectral Green's function in the energy domain. The above solution shows that the localized bound state is a superposition of the original system state with all the reservoir states. In this new basis, the total

Hamiltonian under driving can be written as

$$
H_{\text{tot}}(t) = \sum_l \epsilon_l c_l^\dagger c_l + \sum_k \epsilon_k' c_k^\dagger c_k + \delta\epsilon_d(t) \left[\sum_{ll'} \lambda_{ll'} c_l^\dagger c_{l'} \right.
$$

$$
\left. + \sum_{lk} [\lambda_{lk} c_l^\dagger c_k + \text{H.c.}] + \sum_{kk'} \lambda_{kk'} c_k^\dagger c_{k'} \right], \qquad (12)
$$

where the coefficients $\lambda_{ll'}$, λ_{lk}, and $\lambda_{kk'}$ are determined by the transformation in Eq. (11) and can be explicitly written as

$$
\lambda_{ll'} = \sqrt{Z_l Z_{l'}}, \qquad (13a)
$$

$$
\lambda_{lk} = \sqrt{Z_l} V_k U(\epsilon_k), \qquad (13b)
$$

$$
\lambda_{kk'} = V_k^* V_{k'} U^*(\epsilon_k) U(\epsilon_{k'}). \qquad (13c)
$$

As a short summary of this section, we show that the static component of the driving field can enhance or weaken the localized bound-state effect in controlling the decoherence. However, the time-dependent part $\delta\epsilon_d(t)$ plays an intrinsically different role in manipulating the decoherence dynamics. Equation (12) shows explicitly that after the diagonalization, the localized bound state and the continuous states are decoupled so that the localized bound states are dissipationless, which is alternative proof of the dissipationlessness of the localized bound states. However, the driving $\delta\epsilon_d(t)$ applied to the system induces the transitions between the localized bound states and the scattering modes in the total system, as shown explicitly by Eq. (12). This mechanism leads to the formation of sidebands [13,40,73,74]. Naturally, the form of $\delta\epsilon_d(t)$ can heavily influence the dynamics of the localized bound states in the open quantum system. In the following two sections, we shall discuss these effects in the real-time domain. One section is focused on the weak-driving case, while the other is focused on the case of strong driving.

III. WEAK DRIVING FIELD

In the following, we shall illustrate that the behavior of $u(t, t_0)$ is mainly determined by the characteristics of $u_0(t, t_0)$ and the spectrum of the driving field for the weak-driving case. The periodic driving field can always be decomposed as oscillations of different frequencies, i.e.,

$$
\delta\epsilon_d(t) = \sum_{n=1}^\infty [A_n \sin(\omega_n t) + B_n \cos(\omega_n t)], \qquad (14)
$$

where $\omega_n = 2n\pi/T$ and A_n and B_n are the amplitudes of the oscillations. When the driving is weak, i.e., all the coefficients A_n and B_n are small, the effects of many terms in the time-dependent part

$$
\delta\epsilon_d(t) \left[\sum_{ll'} \lambda_{ll'} c_l^\dagger c_{l'} + \sum_{lk} [\lambda_{lk} c_l^\dagger c_k + \text{H.c.}] + \sum_{kk'} \lambda_{kk'} c_k^\dagger c_{k'} \right]
$$

$$
\tag{15}
$$

are negligible because of the energy conservation, which is similar to the case of atom-photon interactions in quantum optics. To be explicit, generally speaking, the terms involving $e^{-i\omega_n t} c_m^\dagger c_{m'}$ or its Hermitian conjugate, with energy values satisfying $\hbar\omega_n = \epsilon_m - \epsilon_{m'}$, play a dominate role in the driving

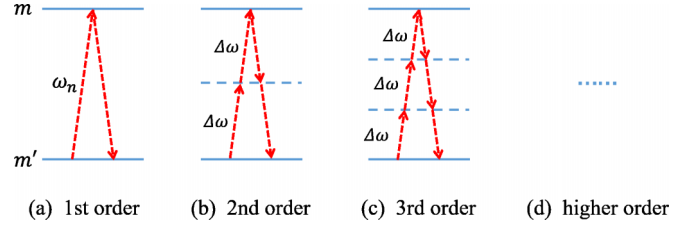(a) 1st order (b) 2nd order (c) 3rd order (d) higher order

FIG. 2. The possible dominate processes involved when the driving is weak; they include (a) the first-order, (b) second-order, (c) third-order, and (d) higher-order processes with energy exchanges of a single quantum, two quanta, three quanta, and more quanta, respectively.

field. These terms represent the process of electron transition between modes m and m' by absorbing energy from or emitting energy to the driving field [see Fig. 2(a)], and m (m') stands for either the localized bound state l or the scattering state k of the reservoir. If no term in Eq. (15) satisfies the above condition, the processes, which are first order, are forbidden. In this case, higher-order processes should be taken into account. For instance, when the driving field $\epsilon_d(t)$ has a single frequency ω and the terms $e^{-i\omega t} c_m^\dagger c_{m'}$ and $e^{i\omega t} c_{m'}^\dagger c_m$, with $\epsilon_m - \epsilon_{m'} = n\hbar\omega$ ($n \neq 1$), exist in the series in Eq. (15), higher-order processes in Figs. 2(b)–2(d) play an important role and determine the main properties of the decoherence dynamics. All these processes in the real-time domain correspond to the formation of sidebands, which effectively modifies the electron tunnelings between the quantum dot and the reservoirs through the driving [13,40,73,74].

In order to demonstrate the above picture of electron transitions between the localized bound states and the scattering states in the reservoir that are induced by the driving, we numerically discuss in the following three different scenarios: (i) no localized bound states, (ii) one localized bound state, and (iii) multiple localized bound states in $u_0(t, t_0)$. Without loss of generality, we use a typical example in which the system-environment interaction is described by the spectral density function [75]

$$
J(\epsilon) = \begin{cases} \eta^2 \sqrt{(2V_0)^2 - (\epsilon - \epsilon_0)^2} & |\epsilon - \epsilon_0| \leqslant 2V_0, \\ 0 & \text{otherwise.} \end{cases} \qquad (16)
$$

This spectral density describes the quantum dot coupling to a reservoir made of a one-dimensional tight-binding chain, with ϵ_0 standing for the on-site electron energy in the chain, V_0 quantifying the electron hopping rate between different sites, and ηV_0 characterizing the system-reservoir coupling strength. Due to the vanishing of the spectral density for $|\epsilon - \epsilon_0| > 2V_0$, there may be zero, one, or two localized bound states in $u_0(t, t_0)$ [15]. In the following, we set $t_0 = 0$ and $\epsilon_0 = 0$, and V_0 is taken as the basic unit. If not otherwise specified, the pulse shape of the driving field $\delta\epsilon_d(t)$ is set as the sinusoidal wave

$$
\delta\epsilon_d(t) = A \sin(2\pi t/T), \qquad (17)
$$

where A denotes the driving-field amplitude and T stands for its fundamental period.

If there is no localized bound state in $u_0(t, t_0)$, no time-dependent localized bound state can be generated by means
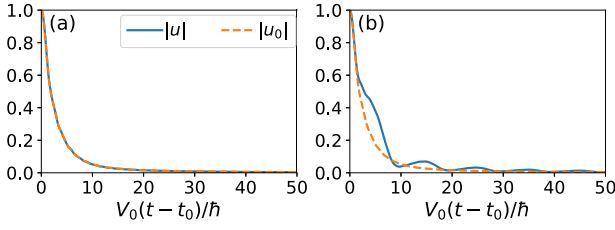
FIG. 3. Plots of $|u_0(t, t_0)|$ and $|u(t, t_0)|$ under periodic driving with different fundamental periods, (a) $T = 1\hbar/V_0$ and (b) $T = 10\hbar/V_0$, in the system-reservoir coupling region in which no localized bound state can exist. The driving fields are both of the sinusoidal type with amplitude $A = 0.5V_0$.

of the periodic drive. In Fig. 3, we set $\eta = 0.8$ and $\overline{\epsilon}_d = V_0$ so that no localized bound state exists in $u_0(t, t_0)$. In Figs. 3(a) and 3(b), the driving field is the sine wave in Eq. (17), with the amplitudes being the same but the fundamental periods varying greatly. When T is short, the influence of the driving is quite limited, such that the evolution of $u(t, t_0)$ is similar to that of $u_0(t, t_0)$ [see Fig. 3(a)]. When T is long, the fundamental frequency $\omega = 2\pi/T$ is much smaller than the bandwidth of the spectral density. As a consequence, many more transitions among the modes in the energy band (in comparison with the short-T case) happen, which makes the driving field exert more influence on the open system dynamics. That is, it induces non-negligible oscillations around $u_0(t, t_0)$ [see Fig. 3(b)]. These oscillations result in positive and negative damping rates in time as a manifestation of the non-Markovian memory effect [15].

In Fig. 4, we set $\eta = 1$ and $\overline{\epsilon}_d = 2.5V_0$, which guarantees one single localized bound state in $u_0(t, t_0)$ (see the solid red lines denoting the localized bound-state energy in the right panels). In Figs. 4(a)–4(d), the pulse shapes are sinusoidal [see Eq. (17)], while in Fig. 4(e), the pulse is a square wave [see Eq. (18)]. From Figs. 4(a)–4(d), the frequency of $\delta\epsilon_d(t)$ increases. In Fig. 4(a), the sideband frequency $\epsilon_l + n\hbar\omega$ (where n is an integer) is not formed [has no overlap with the spectral density function $J(\epsilon)$]; thus, no electron transition can happen between the localized bound state and the continuous band. As a result, the localized bound state is not influenced much by the periodic field, and the dissipationless feature is maintained; that is, $u(t, t_0)$ does not dissipate to zero. In Fig. 4(b), the sideband frequency $\epsilon_l - \hbar\omega$ is formed at the edge of $J(\epsilon)$, which makes the electron in the localized bound state emit an energy $\hbar\omega$ and jump to the continuous energy band. As a result, the driving field generates a dissipation channel, making $u(t, t_0)$ finally decay to zero. However, because the value of the spectral density is small near the band edge, $|u(t, t_0)|$ decays slowly to zero. In Fig. 4(c), the sideband frequency $\epsilon_l - \hbar\omega$ locates in the middle of the reservoir energy band, where the value of the spectral density is large, so that the corresponding dissipation (tunneling) becomes strong. As a result, the electron transits quickly from the localized bound state into the continuous band, and $u(t, t_0)$ decays to zero very quickly, as shown in Fig. 4(c). In Fig. 4(d), the sideband frequency $\epsilon_l - \hbar\omega$ is not in the range of $J(\epsilon)$, but the higher-order sideband frequencies $\epsilon_l - 2\hbar\omega, \ldots, \epsilon_l - 7\hbar\omega$ are formed within the original reser-
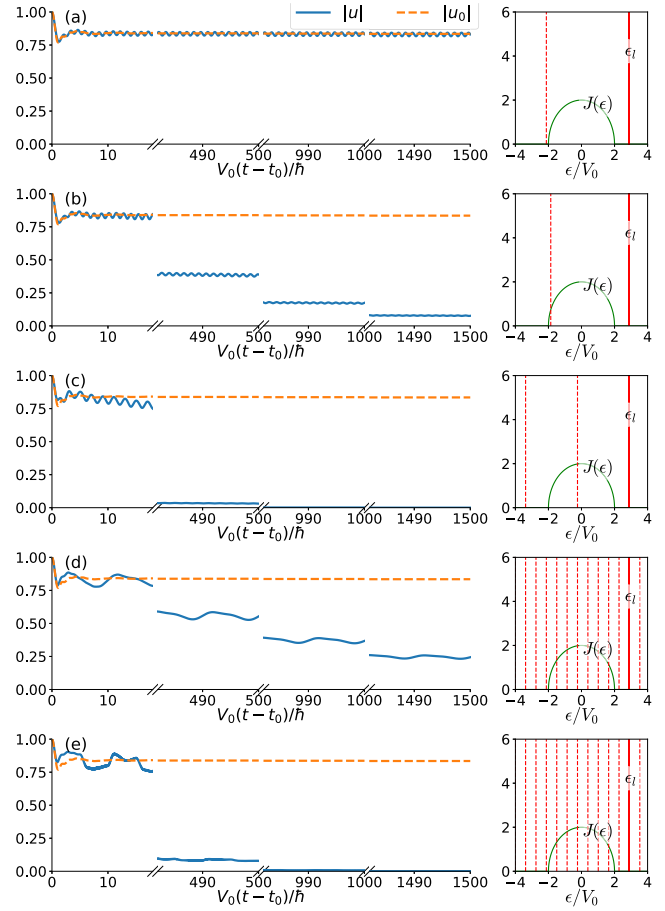

FIG. 4. Plots of $|u_0(t, t_0)|$ and $|u(t, t_0)|$ under a weak sinusoidal-wave driving field with different fundamental periods, (a) $T = 1.25\hbar/V_0$, (b) $T = 1.32\hbar/V_0$, (c) $T = 2\hbar/V_0$, and (d) $T = 10\hbar/V_0$), and (e) the weak square-wave driving field with $T = 10\hbar/V_0$. We also choose the system-reservoir coupling region with only a single localized bound state in the system. The left panels demonstrate the evolution of $|u_0(t, t_0)|$ and $|u(t, t_0)|$, while the right ones are illustrations of the spectra, with the green curve standing for the plot of $J(\epsilon)$ in units of V_0 and the red solid line and red dashed lines being plots of $\epsilon = \epsilon_l$ and the sideband frequency $\epsilon = \epsilon_l + n\hbar\omega$, respectively. (a)–(d) demonstrate typical cases with no sideband, $\epsilon_l + n\hbar\omega$; one sideband, $\epsilon_l - \hbar\omega$, at the edge; the strong sideband, $\epsilon_l - \hbar\omega$; and higher-order sideband frequencies, respectively. In all the plots, the weak-driving-field amplitude $A = 0.5V_0$.

voir spectral density. Consequently, the electron can transit from the localized bound state into the continuous band by emitting subsequently two, three, and four energy quanta and so on due to the driving. This case involves several high-order processes, so $|u(t, t_0)|$ decays gradually with smaller transition rates compared to the case in Fig. 4(c). This picture can be further supported by comparing Fig. 4(e) with Fig. 4(d). In these two plots, parameters A and T are the same, but the driving wave forms are different. In Fig. 4(e), we take $\delta\epsilon_d(t)$ to be a square wave,

$$\delta\epsilon_d(t) = \begin{cases} A & nT \leqslant t \leqslant \left(n + \frac{1}{2}\right)T, \\ -A & \left(n + \frac{1}{2}\right)T \leqslant t \leqslant (n+1)T. \end{cases} \quad (18)$$
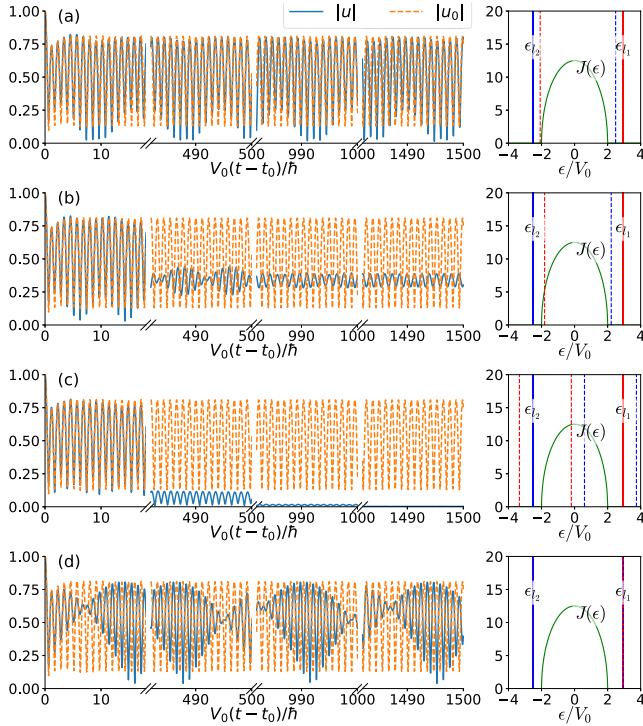
FIG. 5. Plots of $|u_0(t, t_0)|$ and $|u(t, t_0)|$ under a weak driving field with different fundamental periods: (a) $T = 1.25\hbar/V_0$, (b) $T = 1.32\hbar/V_0$, (c) $T = 2\hbar/V_0$, and (d) $T = 2\pi\hbar/(\epsilon_{l_1} - \epsilon_{l_2})$ in the coupling region with multiple localized bound states in the system. The conventions of the plots are the same as those in Fig. 4, except that there are two localized bound states in this case and in the right panels the series of plots $\epsilon = \epsilon_{l_1} + n\hbar\omega$ and $\epsilon = \epsilon_{l_2} + n\hbar\omega$ are colored red (light gray) and blue (dark gray), respectively. From (a) to (c), the fundamental period increases such that in these cases, no sideband frequency, $\epsilon_{l_i} + n\hbar\omega$; a single sideband frequency; and two sideband frequencies formed. In (d), the fundamental frequency is chosen so that ω is exactly the energy difference of the two localized bound states.

Even though the fundamental frequencies are the same, the driving in Eq. (18) possesses sideband frequency components $2\omega, 3\omega, \ldots$, which induces first-order transitions directly. As a result, the decay is much faster than that in Fig. 4(d).

When there are multiple localized bound states in $u_0(t, t_0)$, the phenomena are more abundant. If the localized bound state l_i exists to form sidebands $\epsilon_{l_i} \pm n\hbar\omega$, dissipation induced by the driving must happen. In Fig. 5, we set the parameters $\bar{\epsilon}_d = 0.5V_0$ and $\eta = 2.5$ to generate two localized bound states in $u_0(t, t_0)$, with the energy configuration shown in the right panels. The wave forms of the driving field are all chosen to be sinusoidal. In Fig. 5(a), sideband $\epsilon_{l_i} + n\hbar\omega$ (n can be both positive and negative integers) is not formed. As a result, the localized bound states cannot exchange energy with the continuous reservoir spectrum, making them both isolated, and dissipation does not happen. In other words, the localized bound states can be protected by properly selecting the fundamental frequency of the driving field. In Fig. 5(b), the sideband spectrum series of l_1 are formed; therefore, only l_2 would survive in the long-time limit of $u(t, t_0)$. In Fig. 5(c), the sideband frequencies are valid for both localized bound states.

As a consequence, both localized bound states become dissipative due to the driving, and $u(t, t_0)$ decays quickly to zero. In the special but particularly interesting case in Fig. 5(a), the fundamental frequency of the driving exactly matches the energy difference of the localized bound states, and no sideband is generated. The corresponding dynamics is plotted in Fig. 5(d). As one can see, not only are both the localized bound states protected like those in Fig. 5(a), but an obvious beating character is revealed in the evolution of $u(t, t_0)$. In fact, this could be considered a realization of Rabi oscillation between the two dissipationless localized bound states. It may show a different approach for controlling quantum coherence with the decoherence-free subspace made of localized bound states for quantum information processing.

As a summary of this section, we show that the time-dependent (zero-averaged) part of a weak driving field cannot generate new localized bound states, but it can usually destroy the dissipationlessness of the existing localized bound states. This destructive process is mediated by the energy exchanges between the localized bound state and the continuous energy states of the reservoir through the formation of sidebands so that the localized bound state is no longer isolated. The periodic driving generates sidebands and makes the electrons in the localized bound state absorb or emit energy from the driving field and transit to the continuous states so that dissipative channels are forced to open for the localized bound states as well. However, through proper adjustment of the frequencies of the periodic driving field, the driving field will not cause electron transition to occur between the localized bound state and the continuous energy states. On the contrary, the electrons can periodically oscillate among localized bound state(s) through the driving-field control. This could generate quantum coherence among dissipationless localized bound states and could provide a practically reliable approach for decoherence-free quantum information processing.

IV. STRONG DRIVING FIELD

When the driving field is strong, the dynamical picture of energy transfer seen in the weak driving field is modified. This is clearly revealed by the phenomena shown in Fig. 6. To demonstrate the difference between the dynamics for weak and strong driving fields, we adopt the parameter settings $\eta = 1$ and $\bar{\epsilon}_d = 2.5V_0$ (which are the same as those in Fig. 4) such that only one single localized bound state exists when the driving $\delta\epsilon_d(t)$ is absent.

In Fig. 6, the fields are all in the sine shape with the amplitude set at $A = 5V_0$, which is much larger than those in Fig. 4. The fundamental frequencies in the top two plots are the same as those in Fig. 4. Note that for $T = 1.25\hbar/V_0$, the sidebands $\epsilon_l + n\hbar\omega$ are not formed, so no dissipation channel is opened to the localized bound state, regardless of whether the driving is strong or weak [see Fig. 6(a)]. Although the modulation of the localized bound state is obvious when compared with the dynamics in the weak-driving case, the dissipationless localized bound state is protected. Furthermore, when the sideband $\epsilon_l - \hbar\omega$ forms at the band edge of the reservoir spectrum, the dynamics of the localized bound state is not very different from the case without overlaps with the continuous energy band [compare Figs. 6(a) and 6(b)].
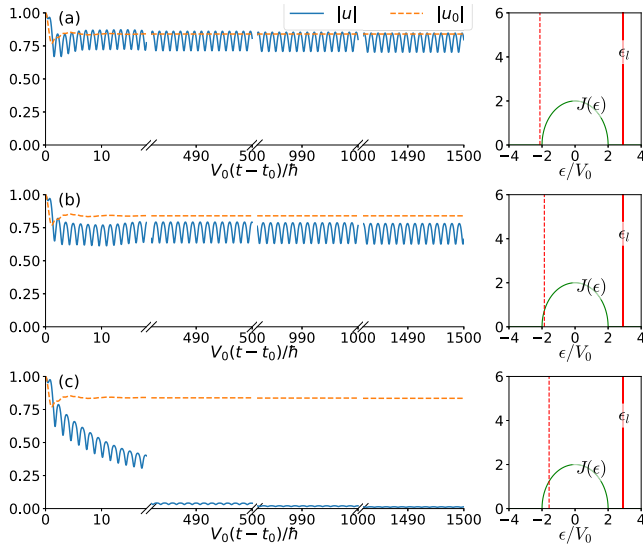
FIG. 6. Plots of $|u_0(t,t_0)|$ and $|u(t,t_0)|$ under a strong driving field with different fundamental periods, (a) $T = 1.25\hbar/V_0$, (b) $T = 1.32\hbar/V_0$, and (c) $T = 1.405\hbar/V_0$, in the coupling region with only one localized bound state in the system. The strong-driving amplitude $A = 5V_0$. The driving field is a sinusoidal wave, and the results demonstrate the cases in which the energy value $\epsilon_l - \hbar\omega$ is around the spectral band edge of the reservoir.

On the other hand, the dynamics of the localized bound state given in Fig. 6(b) is significantly different from the dynamics for the weak driving [compare with Fig. 4(b)]. This shows that for strong driving, even though electrons can transit from the localized bound state to the spectral edge state of the reservoir, no dissipation happens, and the dissipationless localized bound state is well protected, as shown in Fig. 6(b). This is because the dissipation of the spectral edge state of the reservoir is weak (the value of the spectral density is small for the edge states) but the driving field is very strong; as a result, electron transitions between the localized bound state and the reservoir spectral edge state are so fast that electrons do not have enough time to respond to the dissipation into the reservoir with such weak dissipation. This decoherence suppression effect from the strong-driving effect plays a role similar to that in dynamical decoupling protocols [22–27]. This result shows that the picture of electron transitions induced by the driving can be significantly different for the weak and strong driving fields. For strong driving, the dissipationless localized bound state can be protected better.

When the fundamental frequency increases further such that sideband effect with frequency $\epsilon_l - \hbar\omega$ becomes strong [see Fig. 6(c)], the corresponding dissipation for these reservoir states increases significantly. As a result, the dissipationlessness of the localized bound state breaks down because the dissipation time becomes shorter in comparison with the transition time of electrons between the localized bound state and the reservoir states. Then the strong driving field can also result in dissipation. The above results show that strong driving is more feasible for protecting the dissipationlessness

of the localized bound states with the proper selection of the driving-field frequency.

V. DISCUSSION AND CONCLUSION

In this work, we studied the dynamics of dissipationless localized bound states in open quantum systems with periodic driving-field controls. We presented a general picture of electron transitions in the system induced by the driving field and the subsequent decoherence dynamics, which corresponds to sideband generation from the driving. The driving field can be decomposed into the static part and the zero-averaged oscillating part. The static part of the driving can be properly set to manipulate the existence of the dissipationless localized bound states against decoherence, while the zero-averaged part can have totally different effects on the dissipationless localized bound states depending on the formation of sidebands. Specifically, the periodic driving field would usually make the localized bound states decay if sidebands overlapping with the continuous spectra are generated from the driving. With the proper selection of the periodic driving-field frequency, sidebands would not be formed, and the dissipationless localized bound states not only can be protected but also can be manipulated to generate further the quantum coherence between different localized bound states.

The formation of sidebands from the (zero-averaged periodic) driving that induces dissipations is explained with real-time electron transition processes between the localized bound states and the continuous energy states. In the weak-driving case, it shows that if the electron in a localized bound state can absorb or release one or several energy quanta (such as the high-order processes) from the driving field and transits to the continuous energy band, the sidebands can be formed. That is, if $\epsilon_l + n\hbar\omega \in \mathcal{B}$ (n is an integer), where $\mathcal{B}$ stands for the continuous spectrum of the reservoir, then the localized bound states are stimulated to decay. Otherwise, by properly choosing the frequency of the periodic driving field such that $\epsilon_l + n\hbar\omega \notin \mathcal{B}$, namely, no sideband is formed, the dissipationlessness of the localized bound state can be well protected from the driving. Moreover, if one chooses the driving frequency to match the energy difference between the different localized bound states, it can generate quantum coherence between these localized bound states in open quantum systems. This provides a practically reliable scheme for the decoherence-free manipulation of quantum states. For the strong-driving case, such protection and manipulation are even enhanced, as we have demonstrated in the paper.

In the literature, we found that sideband generation could also suppress decoherence; see, for example, the spin decoherence in the quantum-dot system [40]. As we have shown in this work, the dissipation induced by the sidebands can be weakened by making the driving strong and the sidebands overlap with only the edge of the original reservoir energy bands. In spin systems, the spin decoherence given by the dissipation through the original noise channels would be dominated by the dissipation due to the sidebands, which is weak compared to the original spin decoherence and can be considered a decoherence suppression effect. But for localized bound states, which are already dissipationless, there is nothing to suppress. Thus, the aim of the driving control on the

dynamics of localized bound states is to avoid the formation of sidebands from the driving to protect the dissipationlessness of localized bound states and then to generate the quantum coherence between the localized bound states.

The localized bound state of open quantum systems is decoherence free, offering a potential application as a quantum memory protocol, as we showed in a recent work [42]. Using the driving control in nanoelectronic devices, our study reveals that the dissipationlessness of the localized bound states in open quantum systems is sensitively related to the frequency of the periodic driving field and also to the driving strength as well as the structure of the reservoir spectrum (noise spectrum). In particular, with the proper choice of the fundamental frequency ω to avoid sideband generation from the driving, the driving control offers us a different avenue for using dissipationless localized bound states for quantum information storage and manipulation. As a rapidly developing field of solid-state quantum computation, the scheme based on all-electric control of electron charge and spin states in semiconductors is considered promising. The dynamics of dissipationless localized bound states in open quantum systems with periodic driving studied in this work is a simple, but general, solution to the electronic dynamics under control. It could shed light on further experimental developments in related phenomena in the future.

[1] M. A. Nielsen and I. Chuang, *Quantum Computation and Quantum Information* (Cambridge University Press, Cambridge, England, 2002).

[2] I. de Vega and D. Alonso, Rev. Mod. Phys. **89**, 015001 (2017).

[3] W.-M. Zhang, Eur. Phys. J. Spec. Top. **227**, 1849 (2019).

[4] L. Van Hove, Physica (Amsterdam) **21**, 517 (1954).

[5] V. Gorini, A. Kossakowski, and E. C. G. Sudarshan, J. Math. Phys. **17**, 821 (1976).

[6] G. Lindblad, Commun. Math. Phys. **48**, 119 (1976).

[7] S. Nakajima, Prog. Theor. Phys. **20**, 948 (1958).

[8] R. Zwanzig, Int. J. Chem. Phys. **33**, 1338 (1960).

[9] H.-P. Breuer and F. Petruccione, *The Theory of Open Quantum Systems* (Oxford University Press, Oxford, 2002).

[10] A. Caldeira and A. Leggett, Phys. A **121**, 587 (1983).

[11] B. L. Hu, J. P. Paz, and Y. Zhang, Phys. Rev. D **45**, 2843 (1992).

[12] M. W. Y. Tu and W.-M. Zhang, Phys. Rev. B **78**, 235311 (2008).

[13] J. Jin, M. W.-Y. Tu, W.-M. Zhang, and Y. Yan, New J. Phys. **12**, 083013 (2010).

[14] C. U. Lei and W.-M. Zhang, Ann. Phys. (NY) **327**, 1408 (2012).

[15] W.-M. Zhang, P.-Y. Lo, H.-N. Xiong, M. W.-Y. Tu, and F. Nori, Phys. Rev. Lett. **109**, 170402 (2012).

[16] F.-L. Xiong and W.-M. Zhang, Phys. Rev. A **102**, 022215 (2020).

[17] H.-L. Lai, P.-Y. Yang, Y.-W. Huang, and W.-M. Zhang, Phys. Rev. B **97**, 054508 (2018).

[18] Y.-W. Huang, P.-Y. Yang, and W.-M. Zhang, Phys. Rev. B **102**, 165116 (2020).

[19] P.-Y. Yang and W.-M. Zhang, Front. Phys. **12**, 127204 (2017).

[20] E. L. Hahn, Phys. Rev. **80**, 580 (1950).

[21] H. Y. Carr and E. M. Purcell, Phys. Rev. **94**, 630 (1954).

[22] L. Viola and S. Lloyd, Phys. Rev. A **58**, 2733 (1998).

[23] L. Viola, E. Knill, and S. Lloyd, Phys. Rev. Lett. **82**, 2417 (1999).

[24] P. Zanardi, Phys. Rev. A **63**, 012301 (2000).

[25] M. S. Byrd and D. A. Lidar, Phys. Rev. Lett. **89**, 047901 (2002).

[26] L.-A. Wu, M. S. Byrd, and D. A. Lidar, Phys. Rev. Lett. **89**, 127901 (2002).

[27] J. Bylander, S. Gustavsson, F. Yan, F. Yoshihara, K. Harrabi, G. Fitch, D. G. Cory, Y. Nakamura, J.-S. Tsai, and W. D. Oliver, Nat. Phys. **7**, 565 (2011).

[28] J. F. Poyatos, J. I. Cirac, and P. Zoller, Phys. Rev. Lett. **77**, 4728 (1996).

[29] D. Englund, D. Fattal, E. Waks, G. Solomon, B. Zhang, T. Nakaoka, Y. Arakawa, Y. Yamamoto, and J. Vučković, Phys. Rev. Lett. **95**, 013904 (2005).

[30] M. Fujita, S. Takahashi, Y. Tanaka, T. Asano, and S. Noda, Science **308**, 1296 (2005).

[31] M. R. Jorgensen, J. W. Galusha, and M. H. Bartl, Phys. Rev. Lett. **107**, 143902 (2011).

[32] M. D. Leistikow, A. P. Mosk, E. Yeganegi, S. R. Huisman, A. Lagendijk, and W. L. Vos, Phys. Rev. Lett. **107**, 193903 (2011).

[33] A. Metelmann and A. A. Clerk, Phys. Rev. X **5**, 021025 (2015).

[34] F. Grossmann, T. Dittrich, P. Jung, and P. Hänggi, Phys. Rev. Lett. **67**, 516 (1991).

[35] M. Grifoni and P. Hänggi, Phys. Rep. **304**, 229 (1998).

[36] W. D. Oliver, Y. Yu, J. C. Lee, K. K. Berggren, L. S. Levitov, and T. P. Orlando, Science **310**, 1653 (2005).

[37] L. Zhou, S. Yang, Y.-X. Liu, C. P. Sun, and F. Nori, Phys. Rev. A **80**, 062109 (2009).

[38] S.-B. Xue, R.-B. Wu, W.-M. Zhang, J. Zhang, C.-W. Li, and T.-J. Tarn, Phys. Rev. A **86**, 052304 (2012).

[39] X. Luo, L. Li, L. You, and B. Wu, New J. Phys. **16**, 013007 (2014).

[40] J. Jing, P. Huang, and X. Hu, Phys. Rev. A **90**, 022118 (2014).

[41] T. Oka and S. Kitamura, Annu. Rev. Condens. Matter Phys. **10**, 387 (2019).

[42] K.-T. Chiang and W.-M. Zhang, Phys. Rev. A **103**, 013714 (2021).

[43] F. Yan, S. Gustavsson, J. Bylander, X. Jin, F. Yoshihara, D. G. Cory, Y. Nakamura, T. P. Orlando, and W. D. Oliver, Nat. Commun. **4**, 2337 (2013).

[44] F. Yoshihara, Y. Nakamura, F. Yan, S. Gustavsson, J. Bylander, W. D. Oliver, and J.-S. Tsai, Phys. Rev. B **89**, 020503(R) (2014).

[45] T. Nakajima, A. Noiri, K. Kawasaki, J. Yoneda, P. Stano, S. Amaha, T. Otsuka, K. Takeda, M. R. Delbecq, G. Allison, A. Ludwig, A. D. Wieck, D. Loss, and S. Tarucha, Phys. Rev. X **10**, 011060 (2020).

[46] J. Yoneda, K. Takeda, T. Otsuka, T. Nakajima, M. R. Delbecq, G. Allison, T. Honda, T. Kodera, S. Oda, Y. Hoshi, N. Usami, K. M. Itoh, and S. Tarucha, Nat. Nanotechnol. **13**, 102 (2018).

[47] M. Veldhorst, J. C. C. Hwang, C. H. Yang, A. W. Leenstra, B. de Ronde, J. P. Dehollain, J. T. Muhonen, F. E. Hudson, K. M. Itoh, A. Morello, and A. S. Dzurak, Nat. Nanotechnol. **9**, 981 (2014).

[48] K. Eng, T. D. Ladd, A. Smith, M. G. Borselli, A. A. Kiselev, B. H. Fong, K. S. Holabird, T. M. Hazard, B. Huang, P. W. Deelman, I. Milosavljevic, A. E. Schmitz, R. S. Ross, M. F. Gyure, and A. T. Hunter, Sci. Adv. **1**, e1500214 (2015).

[49] A. G. Kofman and G. Kurizki, Phys. Rev. Lett. **87**, 270405 (2001).

[50] G. S. Uhrig, Phys. Rev. Lett. **98**, 100504 (2007).

[51] L. Cywiński, R. M. Lutchyn, C. P. Nave, and S. Das Sarma, Phys. Rev. B **77**, 174509 (2008).

[52] M. J. Biercuk, A. C. Doherty, and H. Uys, J. Phys. B **44**, 154002 (2011).

[53] T. J. Green, J. Sastrawan, H. Uys, and M. J. Biercuk, New J. Phys. **15**, 095004 (2013).

[54] C. Chen, J.-H. An, H.-G. Luo, C. P. Sun, and C. H. Oh, Phys. Rev. A **91**, 052122 (2015).

[55] C. Ma, Y.-S. Wang, and J.-H. An, Phys. Rev. A **97**, 023808 (2018).

[56] S.-Y. Bai, C. Chen, H. Wu, and J.-H. An, Adv. Phys. X **6**, 1870559 (2021).

[57] D. Loss and D. P. DiVincenzo, Phys. Rev. A **57**, 120 (1998).

[58] R. Hanson, L. P. Kouwenhoven, J. R. Petta, S. Tarucha, and L. M. K. Vandersypen, Rev. Mod. Phys. **79**, 1217 (2007).

[59] K. Takeda, A. Noiri, T. Nakajima, J. Yoneda, T. Kobayashi, and S. Tarucha, Nat. Nanotechnol. **16**, 965 (2021).

[60] D. M. Zajac, A. J. Sigillito, M. Russ, F. Borjans, J. M. Taylor, G. Burkard, and J. R. Petta, Science **359**, 439 (2018).

[61] T. F. Watson, S. G. J. Philips, E. Kawakami, D. R. Ward, P. Scarlino, M. Veldhorst, D. E. Savage, M. G. Lagally, M. Friesen, S. N. Coppersmith, M. A. Eriksson, and L. M. K. Vandersypen, Nature (London) **555**, 633 (2018).

[62] W. Huang, C. H. Yang, K. W. Chan, T. Tanttu, B. Hensen, R. C. C. Leon, M. A. Fogarty, J. C. Hwang, F. E. Hudson, K. M. Itoh, A. Morello, A. Laucht, and A. S. Dzurak, Nature (London) **569**, 532 (2019).

[63] Y. He, S. Gorman, D. Keith, L. Kranz, J. Keizer, and M. Simmons, Nature (London) **571**, 371 (2019).

[64] H. Haug and A.-P. Jauho, *Quantum Kinetics in Transport and Optics of Semiconductors* (Springer, New York, 2008), Vol. 2.

[65] M. D. Blumenthal, B. Kaestner, L. Li, S. Giblin, T. Janssen, M. Pepper, D. Anderson, G. Jones, and D. Ritchie, Nat. Phys. **3**, 343 (2007).

[66] A. Fujiwara, K. Nishiguchi, and Y. Ono, Appl. Phys. Lett. **92**, 042102 (2008).

[67] S. Giblin, S. Wright, J. Fletcher, M. Kataoka, M. Pepper, T. Janssen, D. Ritchie, C. Nicoll, D. Anderson, and G. Jones, New J. Phys. **12**, 073013 (2010).

[68] C.-Y. Lin and W.-M. Zhang, Appl. Phys. Lett. **99**, 072105 (2011).

[69] J. Jin, M. W.-Y. Tu, N.-E. Wang, and W.-M. Zhang, J. Chem. Phys. **139**, 064706 (2013).

[70] M. G. House, I. Bartlett, P. Pakkiam, M. Koch, E. Peretz, J. van der Heijden, T. Kobayashi, S. Rogge, and M. Y. Simmons, Phys. Rev. Appl. **6**, 044016 (2016).

[71] A. Schiller and S. Hershfield, Phys. Rev. B **58**, 14978 (1998).

[72] P.-Y. Yang, C.-Y. Lin, and W.-M. Zhang, Phys. Rev. B **92**, 165403 (2015).

[73] L. P. Kouwenhoven, S. Jauhar, K. McCormick, D. Dixon, P. L. McEuen, Y. V. Nazarov, N. C. van der Vaart, and C. T. Foxon, Phys. Rev. B **50**, 2019 (1994).

[74] A. P. Jauho and K. Johnsen, Phys. Rev. Lett. **76**, 4576 (1996).

[75] M.-H. Wu, C. U. Lei, W.-M. Zhang, and H.-N. Xiong, Opt. Express **18**, 18407 (2010).